Published in final edited form as:
J Immunol. 2010 March 1; 184(5): 2677–2685. doi:10.4049/jimmunol.0903274.

Kinetics of Chemokine-Glycosaminoglycan Interactions Control Neutrophil Migration into the Airspaces of the Lungs

Y. Tanino[1,*], **D.R. Coombe**[5,*], **S.E. Gill**[1,3], **W.C. Kett**[5], **O. Kajikawa**[1], **A.E.I. Proudfoot**[6], **T.N.C. Wells**[7], **W.C. Parks**[1,3], **T.N. Wight**[4], **T.R. Martin**[1], and **C.W. Frevert**[1,2,3]

[1]VA Puget Sound Medical Center, and the Division of Pulmonary/Critical Care Medicine, Department of Medicine, at the University of Washington School of Medicine [2]VA Puget Sound Medical Center, and the Division of Pulmonary/Critical Care Medicine, Department of Comparative Medicine, at the University of Washington School of Medicine [3]VA Puget Sound Medical Center, and the Division of Pulmonary/Critical Care Medicine, Center for Lung Biology, at the University of Washington School of Medicine [4]Hope Heart Program at the Benaroya Research Institute at Virginia Mason, Seattle, WA, U.S.A. [5]School of Biomedical Sciences, Curtin Health Innovation Research Institute, Curtin University of Technology, Perth, Australia [6]Merck Serono International S.A., Geneva, Switzerland [7]Medicine for Malaria Venture, Geneva, Switzerland

Abstract

Chemokine-glycosaminoglycan (GAG) interactions are thought to result in the formation of tissue-bound chemokine gradients. We hypothesized that the binding of chemokines to GAGs would increase neutrophil migration towards CXC-chemokines instilled into lungs of mice. To test this hypothesis we compared neutrophil migration towards rhCXCL8 and two mutant forms of CXCL8, which do not bind to heparin immobilized on a sensor chip. Unexpectedly, when instilled into the lungs of mice the CXCL8 mutants recruited more neutrophils than rhCXCL8. The CXCL8 mutants appeared in plasma at significantly higher concentrations and diffused more rapidly across an extracellular matrix *in vitro*. A comparison of the murine CXC-chemokines KC and MIP-2 revealed that KC was more effective in recruiting neutrophils into the lungs than MIP-2. KC appeared in plasma at significantly higher concentrations and diffused more rapidly across an extracellular matrix *in vitro* than MIP-2. In kinetic binding studies, KC, MIP-2, and rhCXCL8 bound heparin differently, with KC associating and dissociating more rapidly from immobilized heparin than the other chemokines. These data suggest that the kinetics of chemokine-GAG interactions contributes to chemokine function in tissues. In the lungs, it appears that chemokines such as CXCL8 or MIP-2, which associate and disassociate slowly from GAGs, form gradients relatively slowly compared to chemokines that either bind GAGs poorly or interact with rapid kinetics. Thus, different types of chemokine gradients may form during an inflammatory response. This suggests a new model whereby GAGs control the spatiotemporal formation of chemokine gradients and neutrophil migration in tissue.

Address correspondence to: Charles W. Frevert, Department of Comparative Medicine, University of Washington School of Medicine, 1959 N.E. Pacific, Campus Box 357190, Seattle WA 98195, Phone: (206) 764-2389, Fax: (206) 768-5289, cfrevert@u.washington.edu.
*These two authors contributed equally to this work

Keywords

chemokine; glycosaminoglycan; kinetics; neutrophil; lungs; inflammation; rodent

INTRODUCTION

CXC-chemokines are important innate host defense molecules that contribute to neutrophil migration and bacterial clearance from the lungs (1–3). They also play a role in processes that are independent of neutrophil recruitment, such as angiogenesis and vascular remodeling (4, 5). CXC-chemokines are implicated in a number of lung diseases, including the acute respiratory distress syndrome (ARDS) and pulmonary fibrosis (5–9), but the mechanisms that regulate the biological activity of CXC-chemokines *in vivo* are not well understood.

The CXC-chemokine, CXCL8/Interleukin-8, is the dominant neutrophil chemoattractant produced by alveolar macrophages stimulated with lipopolysaccharide (10). Mice lack the gene for CXCL8 and the murine CXC-chemokines, KC and macrophage inflammatory protein-2 (MIP-2), are considered functional homologs (8, 11–13). KC and MIP-2 are often referred to as redundant chemokines based on their high degree of shared identity (≈ 66%) and because they bind to the same receptor on neutrophils (Fig. 1) (14, 15).

All chemokines tested to date have a GAG-binding domain. The binding of chemokines to GAGs has been proposed to facilitate both the formation of tissue-bound chemokine gradients and the presentation of chemokines to leukocytes in tissues (16–19). The GAG-binding domain of CXCL8 comprises basic residues located in the proximal loop (K20) and C-terminal α-helix (R60, K64, K67, R68) (Fig. 1) (17). In the lungs, CXCL8 binds the GAGs heparan sulfate and chondroitin sulfate, and these interactions promote the dimerization of CXCL8, thereby increasing the amount of CXCL8 bound in lung tissue (20, 21).

Glycosaminoglycans are linear polymers of repeating disaccharides with a high negative charge imparted by the sulfate and/or carboxyl groups that decorate the saccharide backbone. Sulfation occurs within the Golgi during elongation of the GAG chain, and it is the patterns of sulfation that produce the binding motifs recognized by a variety of proteins, including morphogens, growth factors, adhesion molecules, cytokines, and chemokines (22–24). The binding of CXCL8 to heparan sulfate requires the presence of *N*-, 2-*O*, and 6-*O* sulfate groups(18, 25). Much information about chemokine-GAG interactions has been gained from *in vitro* studies, but less is known about the role of chemokine-GAG interactions in regulating leukocyte migration *in vivo*.

The goal of this study was to determine if the chemotactic activity of CXC-chemokines in the lungs was regulated by modulation of chemokine-GAG interactions. CXCL8 and mutants of CXCL8 and the murine chemokines KC and MIP-2 were used in this study. Surprisingly, CXCL8 mutants, mutated in the GAG-binding domain so as to negate binding to GAGs were significantly better at recruiting neutrophils into the airspaces of the lungs of mice. Mutant CXCL8 appeared to diffuse more rapidly through the tissues *in vivo* and across

an extracellular matrix *in vitro* than wild-type CXCL8. A comparison of KC and MIP-2 revealed that KC was significantly more effective in recruiting neutrophils into the lungs than MIP-2, and KC appeared at significantly higher concentrations in plasma and diffused more rapidly across an extracellular matrix *in vitro* than MIP-2. These data and the binding kinetics displayed by MIP-2 and KC interactions with heparin suggest that the kinetics of chemokine-GAG interactions control the spatiotemporal formation of chemokine gradients and hence neutrophil migration into the lungs. Moreover, the differential binding of CXC-chemokines to GAGs in tissue is a mechanism that confers non-overlapping functions to otherwise redundant chemotactic factors.

MATERIALS AND METHODS

Reagents

Recombinant human CXCL8 (rhCXCL8), the single amino acid mutant, R68A-CXCL8, and the triple amino acid mutant, K64A/K67A/R68A-CXCL8 (TM-CXCL8) were obtained from the Pharmaceutical Research Laboratory (A. P. and T.N.C.W., Geneva, Switzerland). In all cases the indicated basic residues were mutated to alanine. Recombinant murine KC and MIP-2 were purchased from Peprotech (Rocky Hill, NJ). Immunoassays specific for human CXCL8, murine KC, and murine MIP-2 were purchased as DuoSets from R&D Systems Inc (Minneapolis, MN). Wild-type CHO cells (CCL-61) and mutant CHO cells (lacking xylosyltransferase; CRL-2242) were purchased from ATCC. A phycoerythrin conjugated murine anti-human CXCL8 monoclonal antibody (Clone 6217) was purchased from R&D Systems, Inc (Minneapolis, MN). Extracellular matrix from Engelbreth Holm-Swarm mouse sarcoma cell line was purchased from Sigma-Aldrich (St. Louis, MO). Enoxaparin sodium (Lovenox®), a low molecular weight heparin (LMWH), was obtained either from Sanofi-Aventis (Bridgewater, NJ) or the pharmacy at Royal Perth Hospital, Perth, Australia. Chondroitin-4-sulfate from bovine trachea, dermatan sulfate from porcine skin, and chondroitin-6-sulfate from shark cartilage all were purchased from Sigma-Aldrich (St. Louis, MO).

Measurement of Lipopolysaccharide

The concentration of lipopolysaccharide was measured by the Limulus amoebocyte lysate test (LAL, Cambrex, MD) according to the manufacture's protocol. This assay was used to show that the different forms of CXCL8 were not contaminated with lipopolysaccharide (data not shown).

Measurement of Neutrophil Chemotaxis *in vitro*

Neutrophil chemotaxis toward recombinant human CXCL8 was measured using a fluorescence-based microchemotaxis assay with human neutrophils as previously described (26). Human neutrophils were recovered from the peripheral blood of healthy volunteers using a density gradient (Lympholyte-poly, Cedarlane Laboratories, Hornby, Canada). After isolation, neutrophils were labeled with calcein-AM [5 μg/ml] (Molecular Probes, Eugene, OR) for 30 minutes, washed two times in phosphate buffered saline (PBS) and resuspended at a concentration of 3×10^6/ml. Briefly, the wells of a 96-well plate were filled with CXCL8 at various concentrations. Polycarbonate filter (8 μm pores) chambers were placed

on the 96-well plate and calcein-labeled neutrophils were added to the top chamber. The chemotaxis chamber, consisting of the filter chambers and 96-well plate, was incubated for 30 min (37° C and 5% CO2). Non-migrating neutrophils were removed from the upper side of the filter. The chemotaxis chamber was placed in a multi-well fluorescent plate reader (CytoFluor II, PerSeptive Biosystems, Framingham, MA) and the migrated cells were measured using the calcein fluorescence signal (excitation − 485 nm, emission − 530 nm). Neutrophil migration was expressed as a percent of the total number of neutrophils that were placed on the topside of the filter (% Total).

Animal Protocols

The Animal Research Committee of the Veterans Affairs Puget Sound Health Care System approved all experiments. C57BL/6 male mice of 7–8 weeks age were purchased from Jackson Laboratories (Bar Harbor, ME) and housed in the animal facility until the day of the experiment. Mice were anesthetized with 3–4% isoflurane and either phosphate buffered saline (PBS) or the CXC-chemokines were instilled into the lungs via direct orotracheal intubation. The mice were allowed to recover from anesthesia and returned to a cage, where they were allowed free access to food and water for the remainder of the study. Mice were euthanized with an overdose of intraperitoneal pentobarbital (120 ng/ml) at specified times.

Isolation of Mouse Bone Marrow Derived Neutrophils

Mice were euthanized by exposure to CO_2 followed by cervical dislocation. The femur and tibia of both hind legs were isolated and freed of all soft tissue, and then both ends of each bone were removed. Each bone was placed proximal end down in a 0.6 mL Eppendorf tube, which had been punctured at its lower tip with an 18-gauge needle and placed inside a 1.5mL Eppendorf tube. The tubes were spun at 3000 X g for 30 seconds and neutrophils were then isolated from the bone marrow cells as previously described (27). Isolated murine neutrophils (at a concentration of 1×10^6/ml) were used for *in vitro* chemotaxis assays as described above for human neutrophils.

Bronchoalveolar Lavage

Bronchoalveolar lavage (BAL) was performed using 0.9% NaCl containing 0.6 mM EDTA. The first lavage was performed using 0.6 ml of fluid followed by three lavages with 0.5 ml. The BAL fluids were mixed, and an aliquot was immediately processed for total and differential cell counts. The remainder of the BAL fluid was spun at 200 x *g* to pellet cells, and the supernatants were stored in individual aliquots at −70° C.

Total and Differential Cell Counts

Total and differential cell counts were performed on BAL fluid. The BAL samples were diluted with trypan blue to determine viability and with crystal violet containing citric acid to measure total leukocyte numbers using a hemacytometer. Differential cell counts were performed on cytocentrifuge preparations stained with Diff-Quik (American Scientific Products, McGaw Park, IL). A minimum of 100 cells were counted for the differential cell counts.

Measurement of Chemokines

The concentration of human CXCL8, murine KC and MIP-2 in plasma was measured with ELISA kits (DuoSet ELISA development kit, R&D, MN) according to the manufacturer's protocols. The lower detection limits were approximately 3.0 pg/ml for each chemokine tested.

Measurement of Chemokine Diffusion *in vitro*

The diffusion of CXC-chemokines across an extracellular matrix was measured using 6.5 mm-diameter, 0.4 μm pore size polycarbonate membrane Transwell plates (Corning, NY). The topside of the filter was coated with 40 μl of extracellular matrix from Engelbreth-Holm-Swarm Mouse Sarcoma (Sigma, MO) diluted with DMEM at the ratio of 1:2. The CXC-chemokines were diluted in PBS containing 0.1% human serum albumin (HSA) and placed in the upper chamber and PBS containing 0.1% HSA was placed in the lower well. The transwells were incubated for 2 h at 37°C, and the chemokine concentrations were measured in the lower wells using specific immunoassays. On occasion LMWH (100 μg/ml) was added to the chemokines before their addition to the top chamber. Dextran labeled with Texas red (10,000 MW, Molecular Probe, OR) was placed in the upper chamber at the same concentration as the chemokines. The amount of dextran in the bottom wells was measured to ensure the integrity of the matrix barrier was similar across all wells.

Analysis of Chemokine Binding to Heparin with Surface Plasmon Resonance

The binding of the chemokines to heparin was analyzed with surface plasmon resonance (SPR) as previously described (28, 29). In addition, to reduce the binding of the proteins to the control surfaces, CM-4 sensor chips (BIAcore, Melbourne, Australia) were coated with streptavidin according to the manufacturer's instructions. Subsequently, biotinylated heparin was immobilized on sensor chips pre-coated with streptavidin, and real-time biomolecular interaction analyses were performed with a BIAcore 2000 SPR biosensor. For direct binding experiments, 74 RU of heparin was immobilized. The three forms of CXCL8, KC and MIP-2 were diluted in running buffer (10 mM HEPES, 150 mM NaCl, 3mM EDTA, 0.005% Tween-20, pH 7.4) at various concentrations (0.15 to 1000 nM) and injected onto the heparinized surfaces at a flow rate of 30 μl/min for 140 seconds. The flow rate was selected to ensure the binding observed was free of mass transfer effects. Running buffer without the CXC-chemokines was then passed over the BIAcore sensor surface. The temperature of the flow cell was maintained at 25° C. The interactions of CXCL8, KC, and MIP-2 with heparin immobilized on the sensor chips were measured in resonance units (RU). Binding was calculated by subtracting the reference signal from a control surface that had been prepared by binding biotin to the streptavidin-coated surface. Between sample runs, the surfaces were regenerated by 50 μl injections of 0.1 M glycine, 1 M NaCl, 0.1% Tween-20, pH 9.5.

For the inhibition of binding experiments a BIAcore SA chip with 740–800 RU of heparin was used. An aliquot (100 μl) of protein (100 nM) was placed into BIAcore autosampler vials and 10 μl of either binding buffer or inhibitor solutions (prepared in binding buffer) was added. Samples were incubated at room temp until injection. The IC_{50} values were determined by curve fitting with Sigma Plot (Systat Software, San Jose) using data from 3

independent experiments all of which were performed using the same heparin coupled biosensor chip.

The potential for aggregation and oligomerization of the proteins was examined by sizeexclusion chromatography using a 30 × 3mm, Superdex 75 column (Amersham Biosciences, Sydney, Australia) fitted to a SMART HPLC system. The column was eluted with PBS at a flow rate of 50 μl/min and the eluent was monitored at 214 nm. The column was calibrated with standard molecular weight markers. Chromatograms indicated that the proteins were homodimers with no evidence of oligomerization.

Flow Cytometric Analysis of CXCL8 Binding to Chinese Hamster Ovary (CHO) Cells

CHO wild-type (WT) and CHO mutant cells (MUT), which lack xylosyltransferase, were plated in growth media (Ham's F-12 media, 10% fetal bovine serum, 0.1% w/v sodium bicarbonate, 1 mM L-glutamine, 10 μL/mL penicillin-streptomycin, 5 μL/mL Amphotericin B) for 2 days. The WT and MUT CHO cells were detached with 2 mM EDTA in PBS, washed twice with ice-cold binding buffer (RPMI 1640, 20 mM Hepes, 1% bovine serum albumin) and then resuspended and incubated with PBS or 700 nM rhCXCL8, R68A-CXCL8, or TM-CXCL8 in a total volume of 200 μL. Cells were incubated on ice for 90 minutes and washed 3 times with binding buffer. This was followed by incubation with a phycoerythrin conjugated murine anti-human CXCL8 monoclonal antibody at a concentration of 2.5 μg/mL diluted in PBS and 1% bovine serum albumin (BSA). Cells were washed 3 times in PBS/1% BSA and analyzed in a Beckman Coulter FC500 using CXP Software (Beckman Coulter, Fullerton, CA).

Statistical Analysis

Nonlinear regression of log transformed and normalized dose response curves was performed to calculate the EC50 and differences in neutrophil chemotaxis towards the three forms of CXCL8 ($p < 0.05$). Differences among groups were determined using one-way ANOVA and comparisons between two samples were performed using the Mann-Whitney U Test ($p < 0.05$). Values are means ± SEM unless otherwise specified.

RESULTS

Neutrophil Migration toward rhCXCL8 and two CXCL8 mutants *in vitro*

The relative chemotactic efficacies of rhCXCL8 and two CXCL8 mutants containing site-specific mutations in the GAG-binding domain (Fig. 1) were measured in an *in vitro* assay. Interestingly, rhCXCL8 and R68A-CXCL8 were equally effective in promoting the migration of human neutrophils *in vitro* (Fig. 2A). In contrast, the dose response curve of TM-CXCL8 (the triple mutant K64A/K67A/R68A) for human neutrophils indicated that this form of CXCL8 had less chemotactic activity for neutrophils *in vitro* ($p < 0.05$). This difference is indicated by EC50 values of 8.14×10^{-10} M, 1.02×10^{-9} M, and 2.81×10^{-9} M for rhCXCL8, R68A-CXCL8, and TM-CXCL8 respectively. Chemotactic assays were performed to measure the migration of bone marrow derived mouse neutrophils towards all three forms of CXCL8. These studies showed that mouse neutrophils had similar chemotactic activity towards rhCXCL8 and the two mutant forms of CXCL8 *in vitro* (data

not shown). Based on these findings we expected that rhCXCL8 would be a more effective neutrophil chemotactic factor in the lungs of mice.

Biological Effects of the Three Forms of CXCL8 in Murine Lungs

To determine the role of the GAG-binding domain of CXCL8 in controlling CXCL8 chemotactic activity *in vivo*, we instilled wild-type and the two mutant CXCL8 into the lungs of mice. Previous studies demonstrated that murine neutrophils migrate towards rhCXCL8 *in vitro* and *in vivo* (11, 12, 15, 30). Initial dose response studies showed peak neutrophil recruitment at 1 μM rhCXCL8 (data not shown); therefore, 1 μM of all three forms of CXCL8 was used for further work. The results of the study were unexpected: the two CXCL8 mutants, R68A-CXCL8, and TM-CXCL8, induced significantly more neutrophil migration into the airspaces of the lungs at 2, 6, and 14 h after intratracheal instillation (Fig. 2B). These data show that the mutation of a single amino acid in the GAG-binding domain of CXCL8, which does not affect neutrophil chemotaxis *in vitro*, significantly increases the biological activity of this chemokine in the lungs. In contrast, there was no difference in the recovery of either alveolar macrophages or lymphocytes when the three mutant forms of CXCL8 were compared (data not shown).

Measurement of CXCL8 in Plasma

To determine if mutations in the GAG-binding domain of CXCL8 altered the movement of CXCL8 from the airspaces of the lungs into the systemic circulation, the three forms of CXCL8 were measured in plasma at 1 and 2 h after their instillation into the lungs of mice. The amount of CXCL8 in plasma increased rapidly with detectable amounts recovered 1 h after the instillation of each of the three forms of CXCL8 (Fig. 3A). Higher levels of R68A-CXCL8 and TM-CXCL8 were detected in plasma at 1 and 2 h as compared with the wild-type CXCL8. This indicates that mutations in the GAG-binding domain of CXCL8 result in a significant increase in the amount of mutant CXCL8 in the systemic circulation.

Diffusion of CXCL8 across an Extracellular Matrix *in vitro*

If binding of CXCL8 to GAGs retains CXCL8 in the extracellular matrix, the diffusion of the three forms of CXCL8 across matrigel-coated tissue culture inserts should serve as a quantitative test. Matrigel is a commercial preparation of extracellular matrix from the EHS tumour and it is known to contain heparan sulfate and chondroitin sulfate proteoglycans, which bind CXCL8 in the lungs (21, 31). Matrigel was used to coat the upper surface of transwell filters and CXCL8 movement across this matrix was determined by measuring the amount of CXCL8 in the bottom well 2 h after solutions containing the different forms of CXCL8 were added into the top well. The results in Figure 3B demonstrate that significantly more R68A-CXCL8 and TM-CXCL8 diffused across the Matrigel layer than rhCXCL8, consistent with increased retention of rhCXCL8 in extracellular matrix as a consequence of its interactions with GAGs.

Neutrophil Migration toward KC and MIP-2 Instilled into the Airspaces of the Lungs

The murine CXC-chemokines KC and MIP-2 are considered to be the functional homologues of CXCL8, and preliminary studies suggested differential binding of KC and

MIP-2 to heparin. Accordingly, studies were undertaken to determine if the differential binding of murine KC and MIP-2 to GAGs controlled their chemotactic activity in the lungs and their appearance in plasma. To compare the ability of KC and MIP-2 to promote neutrophil migration into the airspaces of the lungs, mice were treated with increasing concentrations of KC or MIP-2 [0.1 to 2 μM]. After 4 h the mice were euthanized and the number of neutrophils migrating into the lungs was measured. These results show that KC was much more effective than MIP-2 in recruiting neutrophils into the airspaces of the lungs (Fig. 4). There was a significant increase in the number of alveolar macrophages recovered in the BAL fluid of mice treated with MIP-2 ($4.84 \times 10^5 \pm 7.21 \times 10^4$) and KC ($4.03 \times 10^5 \pm 4.90 \times 10^4$) when compared to mice treated with PBS ($2.15 \times 10^5 \pm 2.27 \times 10^4$, $p < 0.05$ as compared to PBS using one-way ANOVA). When the number of alveolar macrophages in BAL fluid of mice treated with KC and MIP-2 were compared, analysis with one-way ANOVA showed no significant differences between these two groups.

To check whether the instillation of KC may have caused an increased expression of MIP-2 the amount of KC and MIP-2 in the BAL fluid of mice treated with PBS, KC, and MIP-2 was measured. These data show that when KC was instilled into the lungs of mice the amount of MIP-2 recovered in the BAL fluid resembled the amount recovered from mice treated with PBS. Likewise, when MIP-2 was instilled into the lungs very little KC was detected in the BAL fluid (data not shown). In contrast, significant quantities of the instilled chemokine were readily detected in both instances.

Measurement of KC and MIP-2 in Plasma and Diffusion *in vitro*

Both KC and MIP-2 appeared in plasma within 4 h after intratracheal instillation into the lungs (Fig. 5A). Significantly more KC, however, was measured in plasma when compared to MIP-2. Because these data suggest that MIP-2 is sequestered into the lungs to a greater extent than KC, we next measured the diffusion of KC and MIP-2 across an extracellular matrix *in vitro* with the same system used for CXCL8. A direct comparison of KC and MIP-2 showed that KC diffused more rapidly across the Matrigel barrier than MIP-2 (Fig. 5B).

Diffusion of KC, MIP-2 and CXCL8 across an Extracellular Matrix *in vitro* Alone or in the Presence of Soluble Heparin

Flaumenhaft et al. (32) have shown that the complex of heparin-FGF-2 diffused more rapidly than FGF-2 alone by increasing the amount of growth factor in the soluble phase. If a similar mechanism were operative in our *in vitro* system, addition of heparin to CXC-chemokines should increase their diffusion across an extracellular matrix *in vitro*. We therefore measured the diffusion of KC, MIP-2, and CXCL8 across matrigel in the presence of LMWH. The addition of LMWH to MIP-2 and rhCXCL8 significantly increased the diffusion of these two chemokines, but not KC, across the Matrigel barrier, even though the molecular weight of the chemokine + LMWH complex is higher than that of chemokine alone (Fig. 5B). These data suggest that the addition of LMWH prevents the sequestration of CXCL8 and MIP-2 in the matrix, which results in soluble heparin-chemokine complexes that diffuse more rapidly.

Analyses of the Binding of the CXC-Chemokines to Immobilized Heparin using SPR

To characterize the interactions of chemokines with heparin, a range of concentrations (0 – 1000 nM) of the three forms of human CXCL8 and the murine chemokines KC and MIP-2 was injected over a sensor chip onto which heparin was immobilized, and chemokine binding was measured by SPR. Whereas the binding of rhCXCL8 to heparin was readily measured (Fig. 6A), the binding of the mutant forms of CXCL8 could not be detected (data not shown). Examination of the sensorgrams for rhCXCL8 (Fig. 6A), MIP-2 (Fig. 6B) and KC (Fig. 6C) shows that the heparin binding characteristics of these three chemokines are significantly different. Overall, the association and disassociation of rhCXCL8 and MIP-2 with heparin was slower than what was observed for KC. Moreover, for KC the association and the dissociation curves are biphasic: very rapid initial rates of association and disassociation are followed by marked reductions in those rates. The magnitude of the SPR response is dependent upon the mass of the entity in the fluid phase. However, because the molecular weights of CXCL8, KC, and MIP-2 are very similar it is possible to use SPR responses to directly compare the amounts of each protein bound to the sensor chip (Fig. 7). The dose-response curves for CXCL8, MIP-2, and KC suggest that at concentrations below 250 nM, the binding of KC to heparin exceeds that of CXCL8 or MIP-2. Saturation of binding was not observed at the concentrations that could be achieved. The SPR response observed at 1 μM suggests that multiple protein molecules can bind a single heparin chain and that MIP-2 bound more extensively to heparin than to KC or CXCL8.

An indication of the affinity of the binding of CXCL8, MIP-2, and KC to heparin was achieved by estimating the amount of exogenous heparin required to inhibit binding to the heparin coupled biosensor surface (Table I). The observed IC_{50} values for heparin binding were 2.5 uM for rhCXCL8, 2.8 μM for MIP-2, and 0.142 μM for KC. The IC_{50} for the low molecular weight heparin was at least 10-fold higher for each of the chemokines studied. The 20-fold difference in the concentration of soluble heparin required to inhibit the binding of MIP-2 or KC to immobilized heparin indicates that MIP-2 and KC have markedly different binding characteristics, even though they are generally considered to be redundant chemokines. Interestingly, the three forms of chondroitin sulfate, A, B and C, were ineffective inhibitors of CXCL8 and MIP-2 binding to immobilized heparin even when used at a concentration of 6 μM (data not shown). Chondroitin sulfate A and C were similarly ineffective inhibitors of KC binding, but chondroitin sulfate B displayed some activity, having an IC_{50} in the order of 3 μM.

An indication of the stoichiometry can be obtained from the known amount of heparin immobilized on the chip and knowledge of the molecular weights of the interacting partners. The RU value reflects both the amount of a molecule bound to the biosensor surface and also the mass of that molecule. A further complication is that carbohydrates generate a lower response than proteins, as the change in the refractive index at the chip surface per mg/ml of carbohydrate is less than that seen with a globular protein. Thus, carbohydrates give 145 RU/mg/ml and proteins 180 RU/mg/ml).

The reasoning is as follows: The heparin used has an average molecular weight of 13,500 Da and ~74 response units (RU) was immobilized. Using MIP-2 (Mol wt = 7,900 Da) as an example, at a concentration of 1μM, 320 RU indicates the amount of MIP-2 bound to the

immobilized heparin. As the molecular weight of heparin is ~1.7x that of MIP-2 to more directly compare the amounts of each molecule on the chip this needs to be taken into account, adjusting for the molecular weight difference (74/1.7 = 43) and correcting in the other direction for the lower overall response of carbohydrates to proteins gives a ratio of one heparin chain to ~5.9 molecules of MIP-2. Similar calculations can be performed for the other chemokines, their molecular weights being 8,500 Da for CXCL8, and 7,800 Da for KC. These calculations similarly indicate more than one chemokine molecule per heparin chain. However, as these calculations are based on estimates and an assumption of monomeric chemokines, the calculated ratios must be viewed simply as an indication rather than a precise figure. Indeed, it matters little as to the absolute value of the stoichiometry, rather the data indicate that more than one chemokine molecule binds a single heparin chain. For these reasons we have deliberately avoided giving absolute ratios of heparin chains to chemokine molecules in the text.

Binding of CXCL8 to GAGs on CHO Cells

To determine the ability of the mutant forms of CXCL8 to bind naturally occurring GAGs on cell surfaces, the binding of the three forms of CXCL8 to GAGs on CHO cells was measured. These studies were performed with wild-type CHO cells and mutant CHO cells that lack xylosyltransferase and therefore do not have heparan sulfate or chondroitin sulfate on their surfaces (33). Flow-cytometry was used to measure the amount of the various forms of CXCL8 bound to the CHO cells. Preliminary work showed that the mAb used bound to an epitope on CXCL8 sufficiently removed from the GAG-binding site to rule out binding interference from the antibody itself. It is clear from Figure 8 that rhCXCL8 bound to the surface of the CHO cells, whereas the R68A-CXCL8 and the TM-CXCL8 did not bind (mean fluorescence 21.6±0.8, 1.5±0, 1.5±0, respectively, Fig. 8A). There was minimal binding of rhCXCL8 (mean fluorescence 2.1±0.1) to the mutant CHO cells that largely lack GAGs on their surfaces (Fig. 8B), indicating that retention of CXCL8 on CHO cell surfaces is due to a specific interaction with cell surface GAGs.

DISCUSSION

This study on the role of GAG binding in the regulation of CXC chemokine activity in tissues began with the hypothesis that the binding of chemokines to GAGs would increase neutrophil migration towards CXC-chemokines instilled into the lungs of mice. Therefore, neutrophil migration towards rhCXCL8 and two forms of CXCL8 with point mutations in the GAG-binding domain of CXCL8 was compared. Our data showed that the CXCL8 mutants caused more neutrophils to migrate into the lungs than the rh CXCL8. The CXCL8 mutants did not bind to heparin immobilized on a sensor chip or to GAGs on CHO cells and this was associated with more rapid diffusion across an extracellular matrix *in vitro* and more rapid appearance in plasma after instillation into the lungs. A comparison of the chemotactic activity of the murine CXC-chemokines MIP-2 and KC revealed that KC was more effective in recruiting neutrophils than MIP-2, and KC appeared in plasma at significantly higher concentrations than MIP-2. Moreover, KC diffused more rapidly across an extracellular matrix *in vitro*. From these data KC appears to behave like the CXCL8 mutants. However, SPR analyses of KC, MIP-2, and CXCL8 interactions with immobilized

heparin indicated that KC did not lack the ability to bind heparin but had a more rapid association and disassociation with heparin. Our work demonstrates: first, that mutant forms of CXCL8, which have significantly reduced GAG-binding capabilities, are effective chemotactic factors if instilled in the lungs, and second, that the different binding kinetics displayed when chemokines bind to GAGs suggests a mechanism whereby chemokine functions are fine tuned in tissue.

Since the first suggestion that tissue-bound (haptotactic) chemokine gradients were responsible for the directed migration of leukocytes, the role of soluble versus tissue-bound gradients in regulating chemokine function *in vivo* has been debated (18, 20, 21, 34–41). The work presented here shows the formation of chemokine gradients in tissue is more complex than was first recognized. Accordingly, we propose that differences in the kinetics of chemokine-GAG interactions control the chemotactic activity of CXC-chemokines in the lungs.

The *in vitro* and *in vivo* comparison of rhCXCL8, MIP-2, and KC, provided useful insights into the influence of GAGs on chemokine activities in lungs. When the *in vitro* and *in vivo* data with rhCXCL8, MIP-2 and KC are compared, it appears as if MIP-2 is mimicking rhCXCL8. For example, rhCXCL8 was a more potent chemotactic factor than TM-CXCL8 *in vitro* (Fig. 2A). Similarly, MIP-2 is a more potent stimulator than KC of murine neutrophil chemotaxis *in vitro* (14). In kinetic binding studies, MIP-2 and rhCXCL8 have similar binding kinetics, which are much slower than the kinetics of KC binding to heparin (Fig. 6). Furthermore, the addition of LMWH to rhCXCL8 and MIP-2 significantly increased their diffusion across an extracellular matrix *in vitro*, whereas the addition of LMWH did not significantly enhance the already rapid diffusion of KC. Moreover, a minor modification to the GAG-binding domain, like the mutation of one arginine to an alanine in CXCL8 (R68A-CXCL8), significantly impacts the biological activity of CXCL8 in lungs. These findings support the idea that differential binding of CXCL8, MIP-2, and KC to GAGs contributes to their different activities *in vivo*.

Our kinetic studies using SPR of chemokine binding to heparin immobilized on a biosensor chip (Fig. 6) revealed that rhCXCL8 and MIP-2 produced similarly shaped binding curves. However, the curves obtained with KC were quite different, with the association and disassociation stages being biphasic: there was a very rapid initial association, followed by a slower association, as well as an initial very rapid disassociation, followed by a slow disassociation. In contrast, MIP-2 and rhCXCL8 bound more slowly to the heparin surface and dissociated much more slowly. These differences are further emphasized by the dose response curves in Figure 7. It is evident that at concentrations below 250 nM more KC binds to the same heparin surface than either MIP-2 or rhCXCL8. Moreover, the inhibition studies indicate that the binding of soluble heparin to KC more readily inhibits its association with heparin on the sensor surface than that seen when similar experiments are performed with MIP-2 and rhCXCL8 (Table I). Clearly, a lack of heparin binding is not the explanation for the *in vivo* data obtained with KC; rather the different kinetics by which the chemokines bind GAGs provides an explanation.

The ability of a chemokine to diffuse across a matrix depends both on its concentration differences on either side of the matrix and on the interaction kinetics it displays for molecules encountered during diffusion. Thus, MIP-2 and rhCXCL8 diffuse slowly across a matrix because they interact with GAGs in the matrix with slow rates of association and disassociation. This creates a gradient that forms gradually across the matrix as molecules dissociate and rebind. In contrast, the SPR analysis of KC binding to heparin indicates that a significant proportion of the molecules are very rapidly associating and disassociating. Hence, when KC diffuses across an extracellular matrix this rapid association and disassociation with heparan sulfate would result in the rapid formation of a gradient. Furthermore, if the concentrations applied to the matrix are sufficient, more KC should diffuse across the matrix layer in a given time than MIP-2 and CXCL8, simply because of the different binding characteristics of these chemokines to GAGs. This is what was observed.

The *in vivo* data suggest similar explanations: when instilled into lungs, KC more rapidly forms a gradient, facilitating more recruitment of neutrophils in the allocated time than with MIP-2. Moreover, because at the concentration instilled into the lungs even MIP-2 can be detected in the plasma, it is not surprising that the amount of KC found in plasma over the same time period is greater. These data imply different roles for KC and MIP-2 in directing neutrophils to sites of inflammation in the lungs. KC may act in the early stages of inflammation to rapidly bring neutrophils into the affected area, whereas the slowly produced, tissue-bound gradient formed by MIP-2 is responsible for sustained neutrophil recruitment in response to prolonged inflammation.

Collectively our findings support a new model of chemokine-regulated neutrophil recruitment in which the differential binding of chemokines to GAGs controls neutrophil migration through lung tissues. Our data suggest chemokines bind to GAGs on cell surfaces and within the extracellular matrix of the alveolar epithelium, and this binding maintains the highest concentration of chemokine closest to its cellular source. As chemokines diffuse through tissue they form gradients, and the rate and characteristics of gradient formation are in part determined by the kinetics of the interactions of the chemokine with GAGs, the affinity of the chemokine-GAG interaction, and the structure of the tissue (42). Other factors likely to contribute to the types of gradients formed are the amounts of chemokines released by cells (43); the oligomerization of some chemokines (facilitated by binding GAGs) (20, 21, 39); structural differences in GAGs located at different tissue sites; other chemokine receptors such as the promiscuous Duffy receptor (44); and molecules that may influence the amount of soluble chemokines in tissues such as matrix metalloproteinases and sulfatases (45, 46). It appears from our data that the complexities of GAG-chemokine interactions produce a variety of different chemokine gradients that regulate the spatiotemporal migration of leukocytes at the various stages of an inflammatory response in the lungs. In the model's simplest version, chemokines that bind to GAGs with high affinity and fast kinetics develop long-range short-lived gradients, whereas chemokines that bind to GAGs with similar affinities but slow kinetics form short-range long-lived gradients.

Whether the model can be extended to tissues of a totally different architecture than the lungs is unclear. A study by McColl et al. showed that MIP-2 is a more potent neutrophil

chemotactic factor than KC in an air-pouch model in the skin of mice (47). Proudfoot and colleagues showed that the binding of CC-chemokines, CCL2, CCL4, and CCL5, to GAGs is required for oligomerization of these chemokines and the recruitment of leukocytes into the peritoneum (41). The differences from one tissue to another suggest that chemokine functions are regulated not only by their ability to bind GAGs but that tissue-specific factors also contribute. For example, in McColl's study neutrophil recruitment was examined after chemokines were injected into an air pouch established in the loose connective tissue of the skin, a relatively poorly vascularized tissue. In this instance a chemokine, like MIP-2, that binds GAGs with a slow dissociation coefficient is less likely to diffuse away from the site of injection allowing it to penetrate the tissue and set up an effective chemotactic gradient. In the second study where chemokines were injected into the peritoneal cavity, a lack of GAG binding ability would cause the chemokines to diffuse throughout the peritoneal cavity without establishing an effective gradient to attract leukocytes from the mesenteric vasculature into the peritoneum. Hence, the finding that the binding of chemokines to GAGs is essential for leukocyte recruitment into the peritoneum is expected.

In contrast, lungs are designed for maximal diffusion and ready penetration of soluble molecules from the airspaces into the vasculature. They are highly vascularized with a large epithelial surface area and small amounts of interstitial tissue separating the alveolar spaces from the blood vessels. The pulmonary circulation has lower blood pressures and flow than that of the systemic circulation suggesting that when a chemokine is delivered into the airspaces of the lungs, the critical chemokine gradient directing neutrophil emigration is one that forms across the alveolar epithelium and into the interstitial tissue underlying the capillaries. When chemokines are instilled into the lungs they would be contained by the alveolar architecture of the lungs where the alveoli are grape-like clusters of sacs that would limit the diffusion of chemokines away from the site of instillation and allow the chemokine to readily enter the tissues. In this instance GAG binding would slow down penetration rather than facilitate it. Hence, when instilled into the alveolar spaces a chemokine, like KC, that binds GAGs with a fast association and a rapid initial disassociation followed by a slower off-rate has ideal kinetics to rapidly establish a stable and effective gradient. Similarly, a non-GAG binding chemokine (e.g. TM-CXCL8) would simply diffuse through the lung tissue to establish a soluble gradient in the interstitial fluids. In contrast, a chemokine like rhCXCL8 would be sequestered by heparan sulfate proteoglycans on the alveolar epithelial cell surfaces and underlying extracellular matrix where it would be retained for longer periods. These conclusions are supported by our data and previously published work (20).

In conclusion, this work provides a more complete understanding of the mechanisms that control the chemotactic activity of CXC-chemokines in tissue. Our findings suggest that the differential binding of chemokines to GAGs in tissue is a mechanism that provides spatiotemporal fine-tuning to the regulation of neutrophil migration in lungs. Moreover, these studies support the interpretation that the kinetics of chemokine-GAGs interactions are a major contributing factor to the type of chemokine gradient that is formed when chemokines bind GAGs in tissues. Data presented also suggest that the differential binding of CXC-chemokines to GAGs in tissue is a mechanism that confers a non-overlapping function to KC and MIP-2, consistent with increasing evidence that these chemokines are

not redundant chemotactic factors (43). Finally, the work presented in this manuscript further highlight the complexities of GAG-chemokine interactions and their contributions to regulating neutrophil recruitment in different tissues, and the difficulty of directly superimposing experimental findings obtained in one tissue onto another and from one chemokine onto another.

Acknowledgments

We would like to thank Dr. Rolf Drivdahl for their thoughtful advice and careful review of this manuscript, and to Kim Ballman, Steve Mongovin, Carl Baker, Amy Koski, and Venus Wong for their expert technical support.

Support for this study was provided by the Medical Research Service of the U.S. Department of Veterans Affairs (CWF and TRM), HL082658 (WCP), and the Canadian Institutes of Health Research (SEG).

REFERENCES

1. Frevert CW, Farone A, Danaee H, Paulauskis JD, Kobzik L. Functional characterization of rat chemokine macrophage inflammatory protein-2. Inflammation. 1995; 19:133–142. [PubMed: 7535749]
2. Jones MR, Simms BT, Lupa MM, Kogan MS, Mizgerd JP. Lung NF-kappaB activation and neutrophil recruitment require IL-1 and TNF receptor signaling during pneumococcal pneumonia. J Immunol. 2005; 175:7530–7535. [PubMed: 16301661]
3. Tsai WC, Strieter RM, Mehrad B, Newstead MW, Zeng X, Standiford TJ. CXC chemokine receptor CXCR2 is essential for protective innate host response in murine Pseudomonas aeruginosa pneumonia. Infect Immun. 2000; 68:4289–4296. [PubMed: 10858247]
4. Belperio JA, Keane MP, Burdick MD, Gomperts B, Xue YY, Hong K, Mestas J, Ardehali A, Mehrad B, Saggar R, Lynch JP, Ross DJ, Strieter RM. Role of CXCR2/CXCR2 ligands in vascular remodeling during bronchiolitis obliterans syndrome. J Clin Invest. 2005; 115:1150–1162. [PubMed: 15864347]
5. Strieter RM, Gomperts BN, Keane MP. The role of CXC chemokines in pulmonary fibrosis. J Clin Invest. 2007; 117:549–556. [PubMed: 17332882]
6. Miller EJ, Cohen AB, Nagao S, Griffith D, Maunder RJ, Martin TR, Weiner-Kronish JP, Sticherling M, Christophers E, Matthay MA. Elevated levels of NAP-1/interleukin-8 are present in the airspaces of patients with the adult respiratory distress syndrome and are associated with increased mortality. Am Rev Respir Dis. 1992; 146:427–432. [PubMed: 1489135]
7. Aggarwal A, Baker CS, Evans TW, Haslam PL. G-CSF and IL-8 but not GM-CSF correlate with severity of pulmonary neutrophilia in acute respiratory distress syndrome. Eur Respir J. 2000; 15:895–901. [PubMed: 10853855]
8. Belperio JA, Keane MP, Burdick MD, Londhe V, Xue YY, Li K, Phillips RJ, Strieter RM. Critical role for CXCR2 and CXCR2 ligands during the pathogenesis of ventilator-induced lung injury. J Clin Invest. 2002; 110:1703–1716. [PubMed: 12464676]
9. Strieter RM, Keane MP, Burdick MD, Sakkour A, Murray LA, Belperio JA. The role of CXCR2/CXCR2 ligands in acute lung injury. Curr Drug Targets Inflamm Allergy. 2005; 4:299–303. [PubMed: 16101537]
10. Goodman RB, Strieter RM, Frevert CW, Cummings CJ, Tekamp-Olson P, Kunkel SL, Walz A, Martin TR. Quantitative comparison of C-X-C chemokines produced by endotoxin-stimulated human alveolar macrophages. Am J Physiol. 1998; 275:L87–95. [PubMed: 9688939]
11. Bozic CR, Gerard NP, Uexkull-Guldenband Cvon, Kolakowski LF Jr, Conklyn MJ, Breslow R, Showell HJ, Gerard C. The murine interleukin 8 type B receptor homologue and its ligands. Expression and biological characterization. J Biol Chem. 1994; 269:29355–29358. [PubMed: 7961909]
12. Bozic CR, Kolakowski LF Jr, Gerard NP, Garcia-Rodriguez C, Uexkull-Guldenband Cvon, Conklyn MJ, Breslow R, Showell HJ, Gerard C. Expression and biologic characterization of the murine chemokine KC. J Immunol. 1995; 154:6048–6057. [PubMed: 7751647]

13. Zlotnik A, Yoshie O, Nomiyama H. The chemokine and chemokine receptor superfamilies and their molecular evolution. Genome biology. 2006; 7:243. [PubMed: 17201934]
14. Lee J, Cacalano G, Camerato T, Toy K, Moore MW, Wood WI. Chemokine binding and activities mediated by the mouse IL-8 receptor. J Immunol. 1995; 155:2158–2164. [PubMed: 7636264]
15. Fan X, Patera AC, Pong-Kennedy A, Deno G, Gonsiorek W, Manfra DJ, Vassileva G, Zeng M, Jackson C, Sullivan L, Sharif-Rodriguez W, Opdenakker G, Damme JVan, Hedrick JA, Lundell D, Lira SA, Hipkin RW. Murine CXCR1 is a functional receptor for GCP-2/CXCL6 AND IL-8/CXCL8. J Biol Chem. 2007; 282:11658–11666. [PubMed: 17197447]
16. Rot A. Neutrophil attractant/activation protein-1 (interleukin-8) induces in vitro neutrophil migration by haptotactic mechanism. Eur J Immunol. 1993; 23:303–306. [PubMed: 8419183]
17. Kuschert GS, Hoogewerf AJ, Proudfoot AE, Chung CW, Cooke RM, Hubbard RE, Wells TN, Sanderson PN. Identification of a glycosaminoglycan binding surface on human interleukin-8. Biochemistry. 1998; 37:11193–11201. [PubMed: 9698365]
18. Kuschert GS, Coulin F, Power CA, Proudfoot AE, Hubbard RE, Hoogewerf AJ, Wells TN. Glycosaminoglycans interact selectively with chemokines and modulate receptor binding and cellular responses. Biochemistry. 1999; 38:12959–12968. [PubMed: 10504268]
19. Lortat-Jacob H, Grosdidier A, Imberty A. Structural diversity of heparan sulfate binding domains in chemokines. Proc Natl Acad Sci USA. 2002; 99:1229–1234. [PubMed: 11830659]
20. Frevert CW, Goodman RB, Kinsella MG, Kajikawa O, Ballman K, Clark-Lewis I, Proudfoot AE, Wells TN, Martin TR. Tissue-Specific Mechanisms Control the Retention of IL-8 in Lungs and Skin. J Immunol. 2002; 168:3550–3556. [PubMed: 11907118]
21. Frevert CW, Kinsella MG, Vathanaprida C, Goodman RB, Baskin DG, Proudfoot A, Wells TN, Wight TN, Martin TR. Binding of interleukin-8 to heparan sulfate and chondroitin sulfate in lung tissue. Am J Respir Cell Mol Biol. 2003; 28:464–472. [PubMed: 12654635]
22. Esko JD, Selleck SB. ORDER OUT OF CHAOS: Assembly of Ligand Binding Sites in Heparan Sulfate. Annu Rev Biochem. 2002; 71:435–471. [PubMed: 12045103]
23. Handel TM, Johnson Z, Crown SE, Lau EK, Proudfoot AE. Regulation of protein function by glycosaminoglycans--as exemplified by chemokines. Annu Rev Biochem. 2005; 74:385–410. [PubMed: 15952892]
24. Taylor KR, Gallo RL. Glycosaminoglycans and their proteoglycans: host-associated molecular patterns for initiation and modulation of inflammation. Faseb J. 2006; 20:9–22. [PubMed: 16394262]
25. Spillmann D, Witt D, Lindahl U. Defining the Interleukin-8-binding Domain of Heparan Sulfate. J Biol Chem. 1998; 273:15487–15493. [PubMed: 9624135]
26. Frevert CW, Wong VA, Goodman RB, Goodwin R, Martin TR. Rapid fluorescence-based measurement of neutrophil migration in vitro. J Immunol Methods. 1998; 213:41–52. [PubMed: 9671124]
27. Boxio R, Bossenmeyer-Pourie C, Steinckwich N, Dournon C, Nusse O. Mouse bone marrow contains large numbers of functionally competent neutrophils. J Leukoc Biol. 2004; 75:604–611. [PubMed: 14694182]
28. Osmond RI, Kett WC, Skett SE, Coombe DR. Protein-heparin interactions measured by BIAcore 2000 are affected by the method of heparin immobilization. Anal Biochem. 2002; 310:199–207. [PubMed: 12423639]
29. Cochran S, Li C, Fairweather JK, Kett WC, Coombe DR, Ferro V. Probing the interactions of phosphosulfomannans with angiogenic growth factors by surface plasmon resonance. J Med Chem. 2003; 46:4601–4608. [PubMed: 14521421]
30. Lee JS, Frevert CW, Wurfel MM, Peiper SC, Wong VA, Ballman KK, Ruzinski JT, Rhim JS, Martin TR, Goodman RB. Duffy Antigen Facilitates Movement of Chemokine Across the Endothelium In Vitro and Promotes Neutrophil Transmigration In Vitro and In Vivo. J Immunol. 2003; 170:5244–5251. [PubMed: 12734373]
31. Couchman JR, Kapoor R, Sthanam M, Wu RR. Perlecan and basement membrane-chondroitin sulfate proteoglycan (bamacan) are two basement membrane chondroitin/dermatan sulfate proteoglycans in the Engelbreth-Holm-Swarm tumor matrix. J Biol Chem. 1996; 271:9595–9602. [PubMed: 8621634]

32. Flaumenhaft R, Moscatelli D, Rifkin DB. Heparin and heparan sulfate increase the radius of diffusion and action of basic fibroblast growth factor. J Cell Biol. 1990; 111:1651–1659. [PubMed: 2170425]
33. Esko JD, Stewart TE, Taylor WH. Animal cell mutants defective in glycosaminoglycan biosynthesis. Proc Natl Acad Sci USA. 1985; 82:3197–3201. [PubMed: 3858816]
34. Rot A. Endothelial cell binding of NAP-1/IL-8: role in neutrophil emigration. Immunol Today. 1992; 13:291–294. [PubMed: 1510812]
35. Webb LM, Ehrengruber MU, Clark LI, Baggiolini M, Rot A. Binding to heparan sulfate or heparin enhances neutrophil responses to interleukin 8. Proc Natl Acad Sci USA. 1993; 90:7158–7162. [PubMed: 8346230]
36. Tanaka Y, Adam DH, Shaw S. Proteoglycans on endothelial cells present adhesioninducing cytokines to leukocytes. Immunology Today. 1993; 14:111–115. [PubMed: 8466625]
37. Tanaka Y, Adams D, Hubscher S, Hirano H, Siebenlist U, Shaw S. T-cell adhesion induced by proteoglycan-immobilized cytokine MIP-1β. Nature. 1993; 361:79–82. [PubMed: 7678446]
38. Middleton J, Neil S, Wintle J, Clark L-I, Moore H, Lam C, Auer M, Hub E, Rot A. Transcytosis and surface presentation of IL-8 by venular endothelial cells. Cell. 1997; 91:385–395. [PubMed: 9363947]
39. Hoogewerf AJ, Kuschert GS, Proudfoot AE, Borlat F, Clark-Lewis I, Power CA, Wells TN. Glycosaminoglycans mediate cell surface oligomerization of chemokines. Biochemistry. 1997; 36:13570–13578. [PubMed: 9354625]
40. Netelenbos T, Zuijderduijn S, Van Den Born J, Kessler FL, Zweegman S, Huijgens PC, Drager AM. Proteoglycans guide SDF-1-induced migration of hematopoietic progenitor cells. J Leukoc Biol. 2002; 72:353–362. [PubMed: 12149427]
41. Proudfoot AEI, Handel TM, Johnson Z, Lau EK, LiWang P, Clark-Lewis I, Borlat F, Wells TNC, Kosco-Vilbois MH. Glycosaminoglycan binding and oligomerization are essential for the in vivo activity of certain chemokines. Proc Natl Acad Sci USA. 2003; 100:1885–1890. [PubMed: 12571364]
42. Lander AD. Morpheus unbound: reimagining the morphogen gradient. Cell. 2007; 128:245–256. [PubMed: 17254964]
43. De Filippo K, Henderson RB, Laschinger M, Hogg N. Neutrophil Chemokines KC and Macrophage-Inflammatory Protein-2 Are Newly Synthesized by Tissue Macrophages Using Distinct TLR Signaling Pathways. J Immunol. 2008; 180:4308–4315. [PubMed: 18322244]
44. Lee JS, Wurfel MM, Matute-Bello G, Frevert CW, Rosengart MR, Ranganathan M, Wong VW, Holden T, Sutlief S, Richmond A, Peiper S, Martin TR. The Duffy antigen modifies systemic and local tissue chemokine responses following lipopolysaccharide stimulation. J Immunol. 2006; 177:8086–8094. [PubMed: 17114483]
45. Li Q, Park PW, Wilson CL, Parks WC. Matrilysin shedding of syndecan-1 regulates chemokine mobilization and transepithelial efflux of neutrophils in acute lung injury. Cell. 2002; 111:635–646. [PubMed: 12464176]
46. Uchimura K, Morimoto-Tomita M, Bistrup A, Li J, Lyon M, Gallagher J, Werb Z, Rosen SD. HSulf-2, an extracellular endoglucosamine-6-sulfatase, selectively mobilizes heparin-bound growth factors and chemokines: effects on VEGF, FGF-1, and SDF-1. BMC Biochem. 2006; 7:2. [PubMed: 16417632]
47. McColl SR, Clark-Lewis I. Inhibition of murine neutrophil recruitment in vivo by CXC chemokine receptor antagonists. J Immunol. 1999; 163:2829–2835. [PubMed: 10453028]

The abbreviations used are

BAL	Bronchoalveolar Lavage
CHO	chinese hamster ovary
CXCL8	Interleukin-8

EDTA	ethylenediaminetetraacetic acid
ELISA	Enzyme-Linked Immunosorbent Assay
K_D	Dissociation constant
Glycosaminoglycans	GAG
HEPES	4-(2-Hydroxyethyl)piperazine-1-ethanesulfonic acid
HPLC	high pressure liquid chromatography
HSA	Human serum albumin
LMWH	low molecular weight heparin
MIP-2	Macrophage inflammatory protein-2
PBS	Phosphate Buffered Saline
rhCXCL8	Recombinant human CXCL8
R68A-CXCL8	Single amino acid mutation (R68A) of the glycosaminoglycan-binding domain of CXCL8
RU	resonance unit
SPR	Surface plasmon resonance
TM-CXCL8	Triple mutant (K64A/K67A/R68A-CXCL8) of the glycosaminoglycan-binding domain of CXCL8

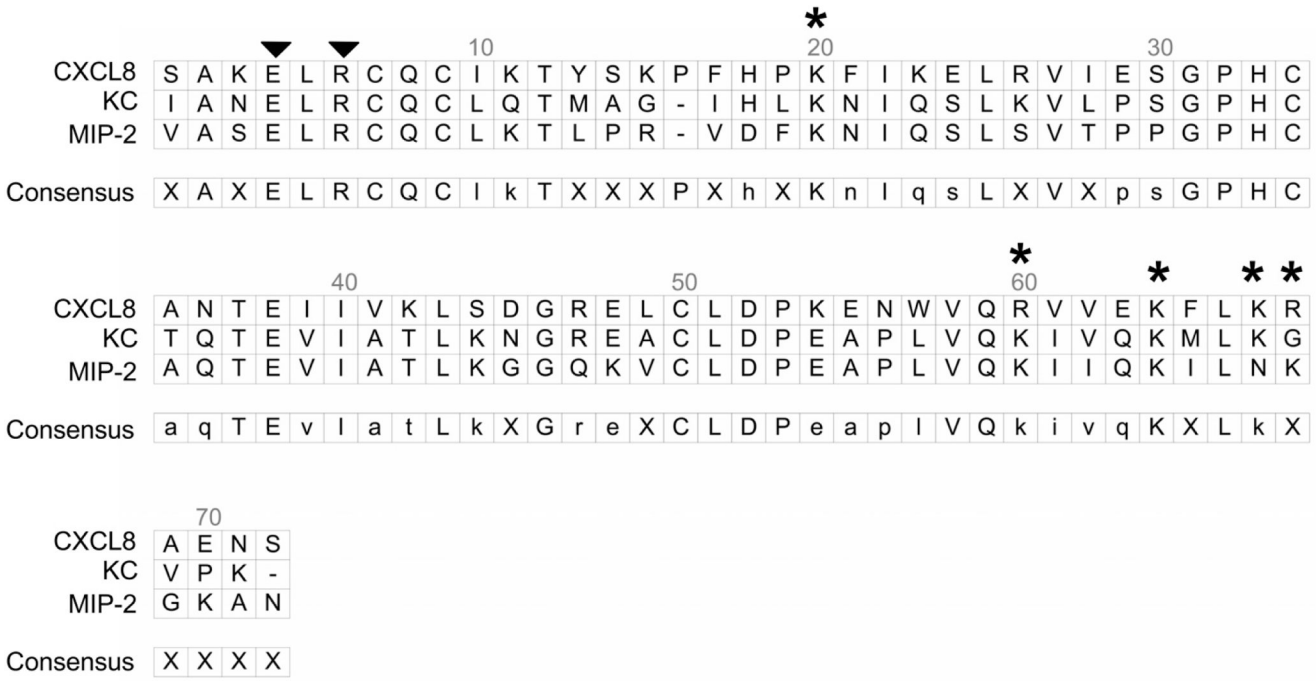

Figure 1.

Alignment of human CXCL8 and the murine CXC chemokines KC and MIP-2. The alignments were performed using DS Gene Software (Accelrys Inc. San Diego, CA). The N-terminal ELR domain, which binds to CXC-receptors on neutrophils, is identified with two arrowheads. Five positively charged amino acids, K20 in the proximal loop, plus R60, K64, K67, and R68 in the C-terminal alpha helix, make up the GAG-binding domain of CXCL8 (17). These five positively charged amino acids are identified with an asterisk (*). Three-dimensional models of CXCL8 show that the proximal loop containing K20 folds to bring this basic residue into close proximity with R60, K64, K67, and R68. The mutant forms of CXCL8 used here are a mutant where arginine at position 68 was converted to an alanine (R68A-CXCL8) and a triplemutant CXCL8 (TM-CXCL8) where lysines at position 64 and 67 and arginine at position 68 were mutated to alanines (K64A/K67A/R68A CXCL8 or TM-CXCL8). Murine KC and MIP-2 have similar three-dimensional structures, suggesting that K20 along with positive amino acids in the C-terminal alpha helix comprise the GAG-binding domains of these two chemokines.

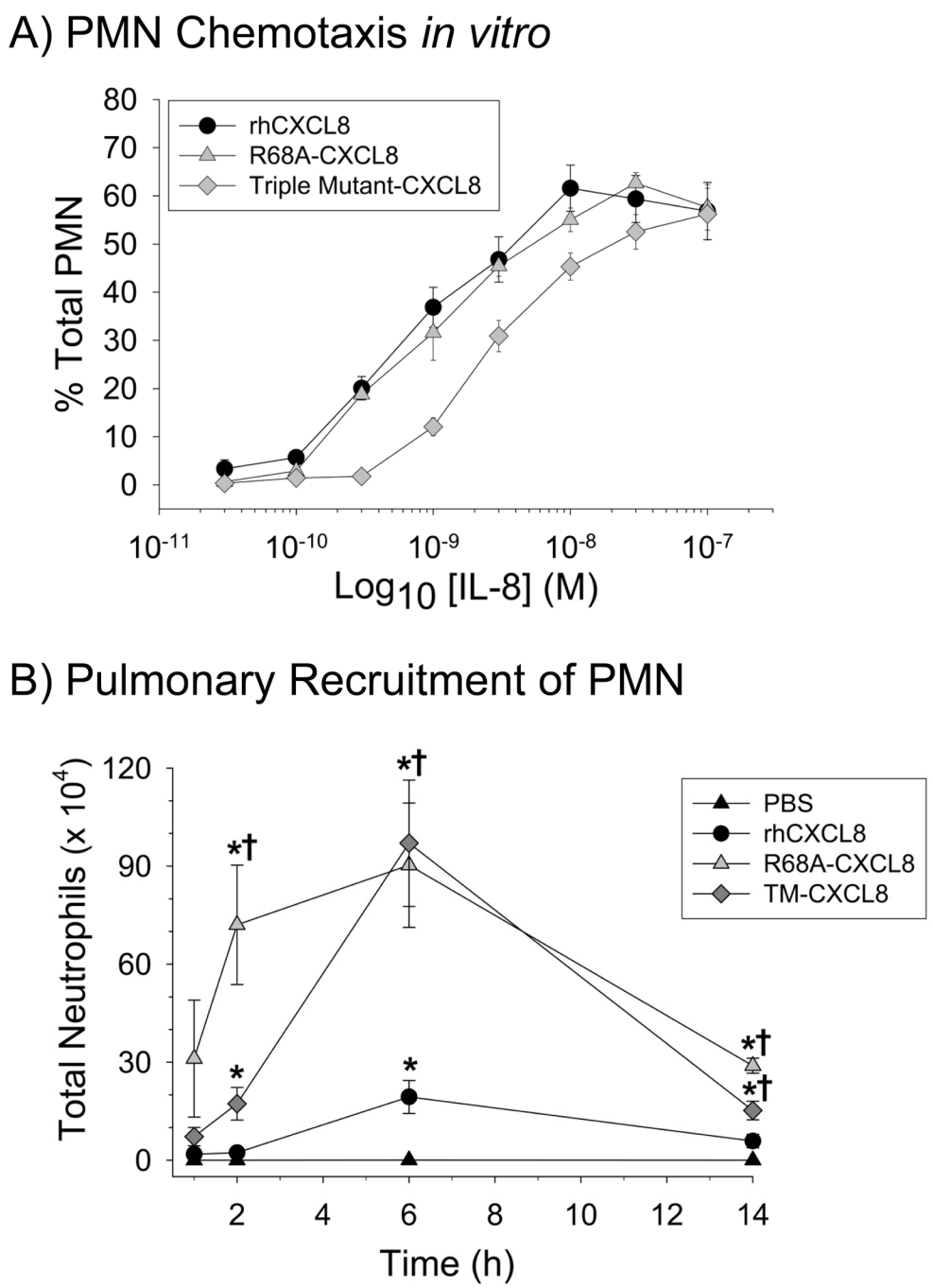

Figure 2.

Neutrophil migration in response to rhCXCL8 and the CXCL8 mutants. (A) Neutrophil migration to the different forms of CXCL8 was measured using fluorescently labeled neutrophils and a Boyden-like chemotaxis chamber. Values are the mean ± SEM, with n = 3 experiments. (B) Neutrophil migration *in vivo* was measured following instillation of either, vehicle (PBS), rhCXCL8, R68A-CXCL8, or TM-CXCL8 into the lungs of mice. All forms of CXCL8 were instilled at 1 μM based on preliminary studies. Necropsies were performed at specified times and the total neutrophils were measured in the BAL fluid. Values are the

means ± SEM with n = 5 to 14 mice/group. Statistical analysis was performed with One-way ANOVA and * is $p < 0.05$ when compared to the vehicle control and † is $p < 0.05$ when compared to rhCXCL8.

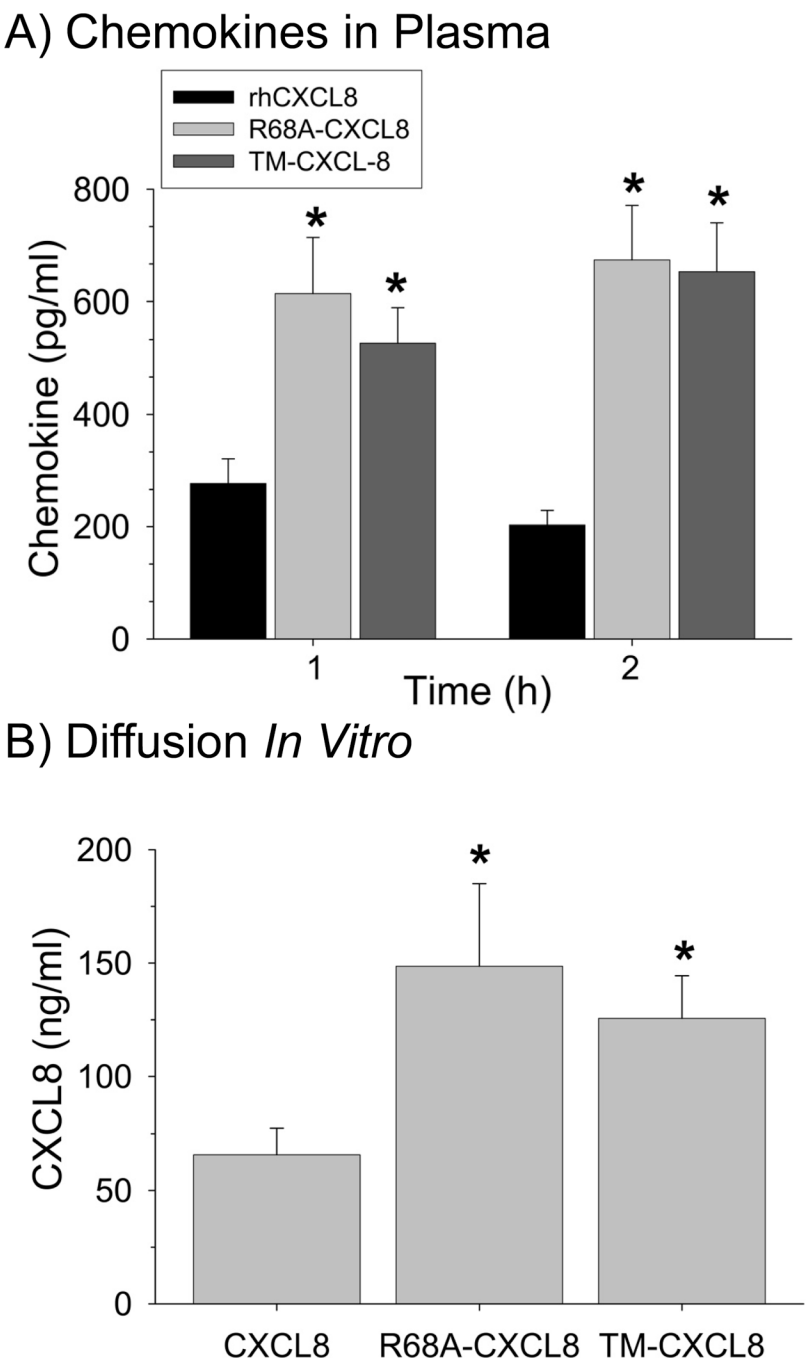

Figure 3.

rhCXCL8 and the CXCL8 mutants diffuse into plasma and across an extracellular matrix at different rates. (A) The amounts of rhCXCL8, R68A-CXCL8 and TM-CXCL8 measured in plasma collected from the mice used in Figure 2B are shown. The three forms of CXCL8 were quantified by ELISA using plasma collected at 1 and 2 h after intratracheal instillation of the chemokines. Values are the means ± SEM with n = 5 to 14 mice/group. (B) The diffusion of the rhCXCL8, R68A-CXCL8, and TM-CXCL8 across an extracellular matrix *in*

vitro. Values are the means ± SEM with n = 7 to 10. Statistical analysis for 3A and 3B was performed with One-way ANOVA and * is $p < 0.05$.

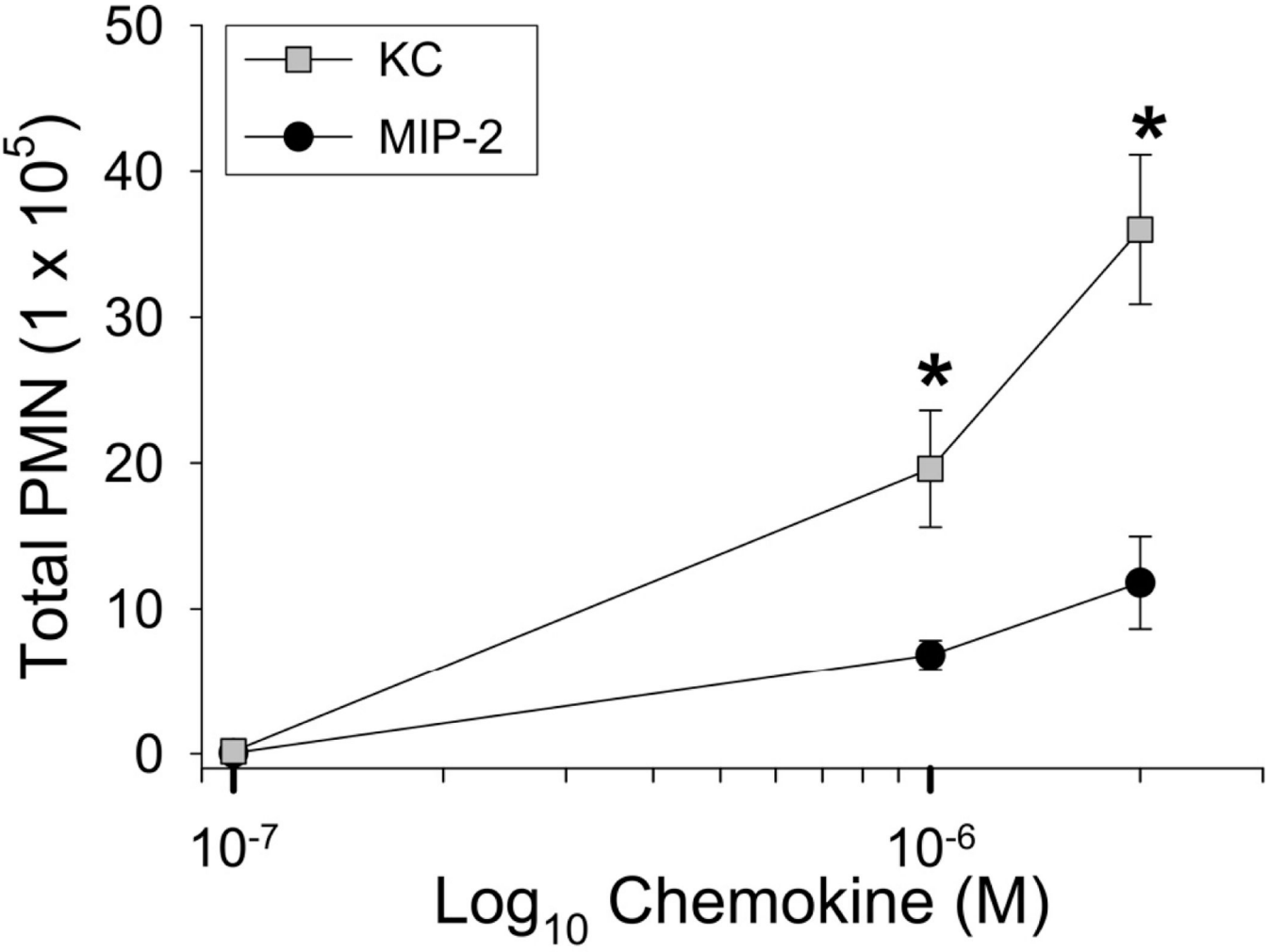

Figure 4.

KC and MIP-2 recruit neutrophils with differing efficacies when instilled into the lungs of mice. KC and MIP-2 were instilled into the lungs of mice at three concentrations (0.1, 1, and 2 μM). Necropsies were performed 4 h after instillation and bronchoalveolar lavage (BAL) was performed to recover cells from the airspaces of the lungs. At each concentration the total number of neutrophils recovered in BAL fluid was determined. Values are the means ± SEM with n = 6 to 9 mice per group. Statistical analysis was performed with Mann-Whitney's U Test and * is $p < 0.05$.

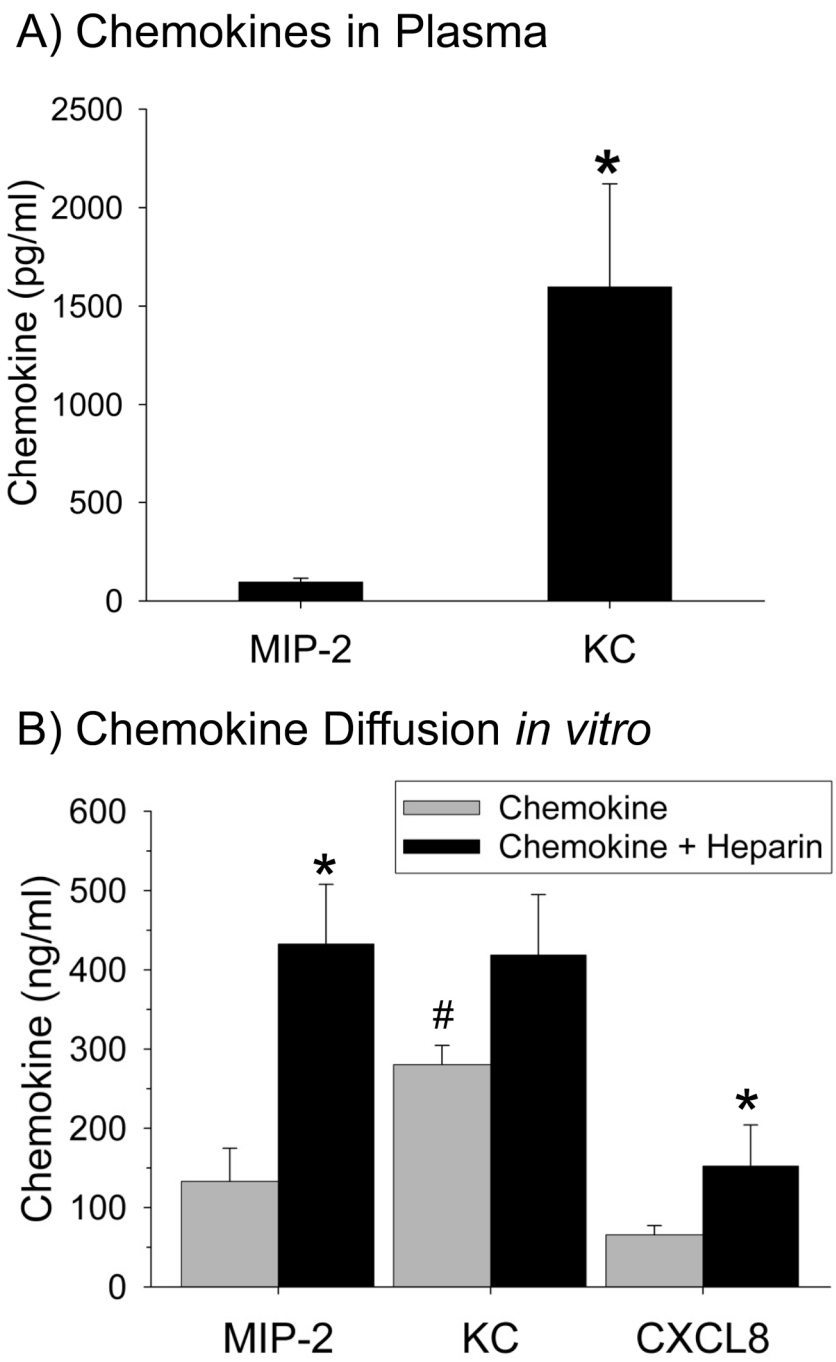

Figure 5.

KC and MIP-2 diffuse into plasma and across an extracellular matrix at different rates. (A) The amount of MIP-2 and KC in plasma was measured using ELISA at 4 h after the intratracheal instillation of the chemokines into the lungs of mice. Values are means ± SEM where n = 5. (B) The diffusion of MIP-2, KC, and CXCL8 across an extracellular matrix was measured in the absence or presence of LMWH *in vitro*. ELISA analyses revealed that there was significantly more KC than MIP-2 in the lower chamber (# is $p < 0.008$). The addition of LMWH significantly increased the recovery of MIP-2 ($p = 0.007$) and CXCL8 (p

= 0.04) but not KC (p = 0.22). * is p < 0.05 when the chemokine alone is compared to the chemokine + LMWH. Statistical analysis was performed with Mann-Whitney's U Test, Values are the means ± SEM with n = 6 to 12.

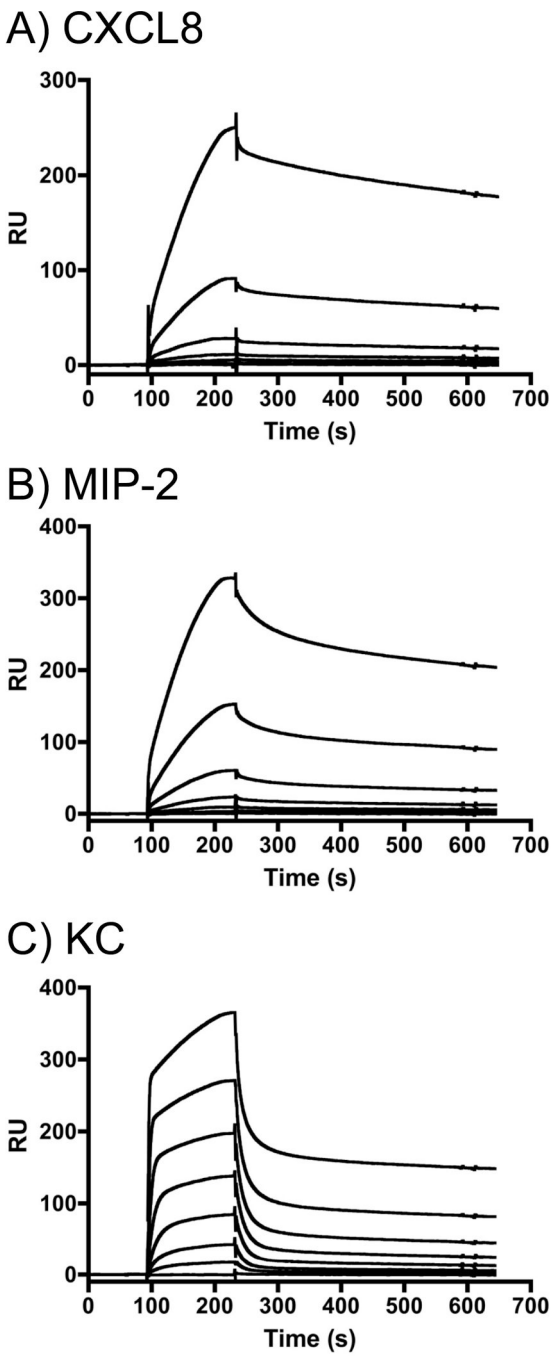

Figure 6.

Sensorgrams obtained used SPR reveal the chemokines bind heparin with different kinetics. The binding of various concentrations of rhCXCL8 (A), MIP-2 (B), and KC (C) to heparinized CM-4 chips is shown. (A) The concentration of rhCXCL8 was (upper to lower curves) 1000 nM, 500 nM, 250 nM, 125 nM, 62.5 nM and 0 nM. (B) The concentrations of MIP-2 were (upper to lower curves) 1000, 333, 111, 37, 12.4, 4.12, nM, (C) The concentrations of KC were (upper to lower curves) 1000, 333, 111, 37, 12.4, 4.12, 1.37, 0.46, 0.15 nM.

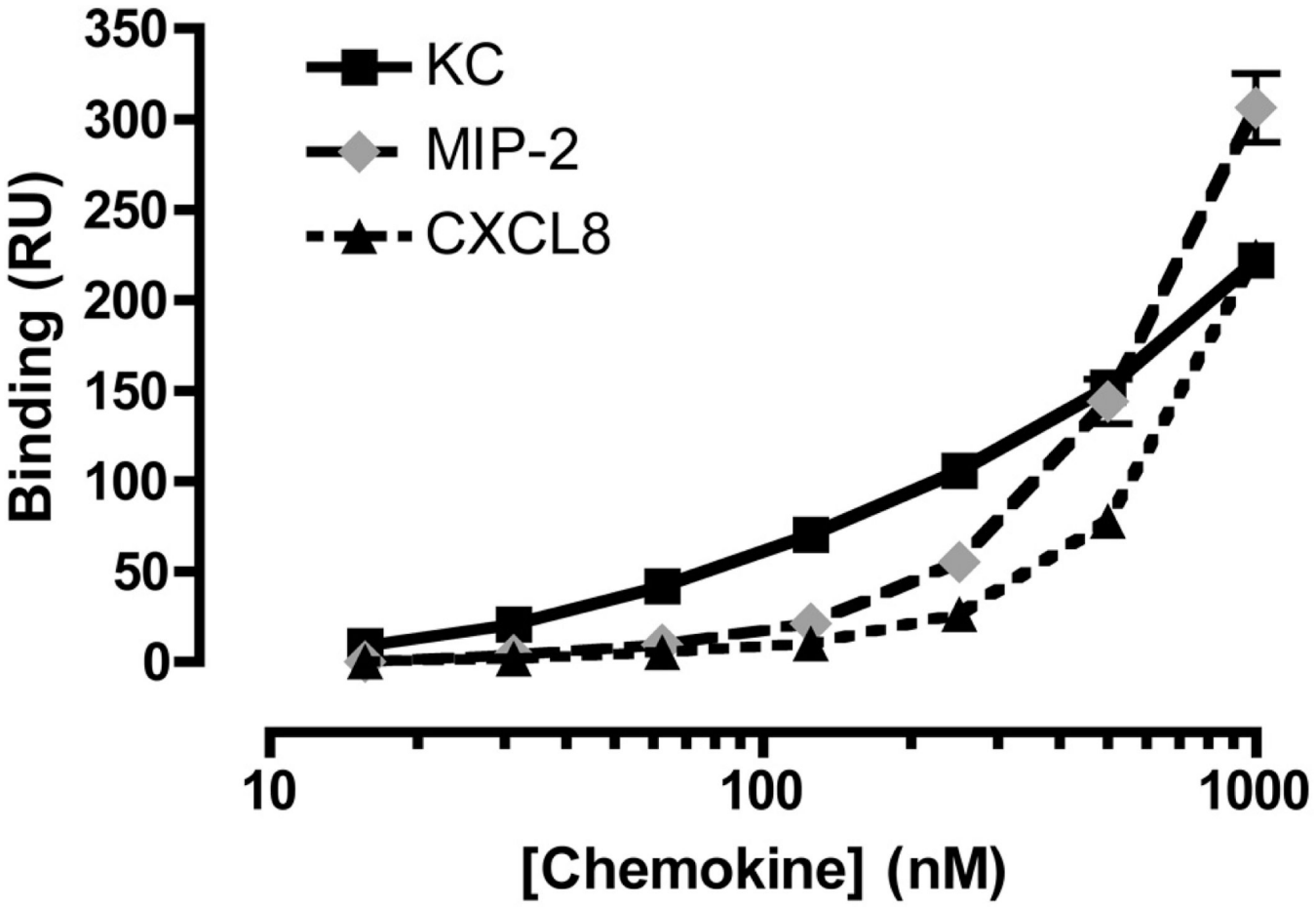

Figure 7.

Dose response curves reveal differences in the binding behavior of the chemokines. The binding of KC (▪, full line), MIP-2 (◆, grey dashed line) and CXCL8 (▲, dotted line) to heparin immobilized on a CM-4 sensor chip is shown. Means and standard errors of the mean are shown, calculated from 3 independent experiments.

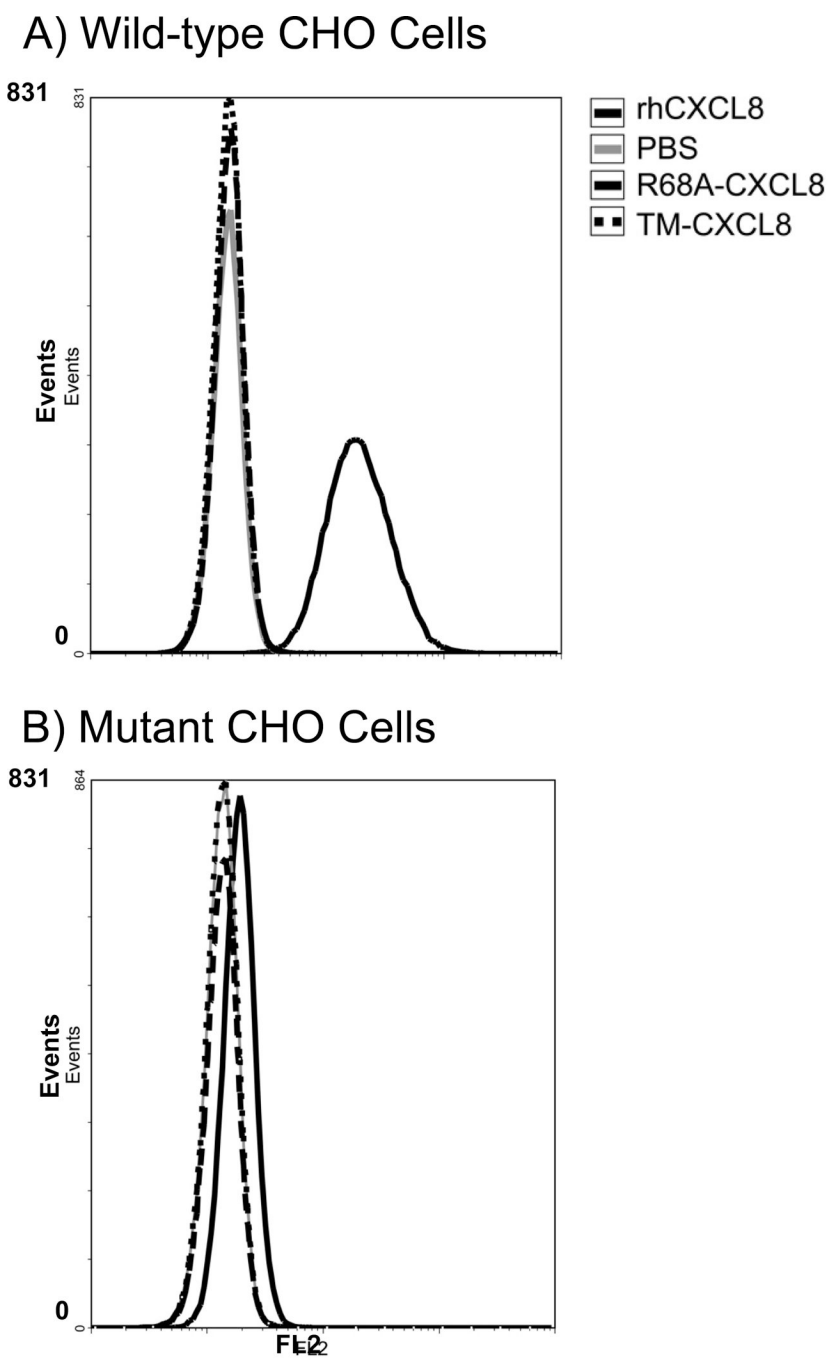

Figure 8.

The binding of the three different forms of CXCL8 [0.70×10^{-6} M] to wild-type (A) and mutant (B) CHO cells was measured by flow cytometry. (A) The binding of rhCXCL8 (black line) R68A-CXCL8 (dashed line) or TM-CXCL8 (dotted line) to wild-type CHO cells. The control was wild-type CHO cells incubated with PBS (grey line). (B) The binding of rhCXCL8 (black line), R68A-CXCL8 (dashed line), or the TM-CXCL8 (dotted line) to

mutant CHO cells lacking xylosyltransferase. The control was mutant CHO cells incubated with PBS (grey line). Shown are representative data of three independent experiments.

Table I

IC_{50} at which soluble heparin and LMWH inhibit chemokine binding to immobilized heparin.

	KC	MIP-2	CXCL8
Heparin	0.142 ± 0.006[1]	2.8 ± 0.45	2.5 ± 0.45
LMWH	3.83 ± 0.9	59.0 ± 9	31.4 ± 0.3

[1] Data represent the concentration (μM) of GAG required to inhibit chemokine (100 nM) binding to heparin immobilized on a sensor surface as determined by SPR. Means ± standard error of the mean are shown for at least 3 independent determinations.